Beaconless Optical Communication System Constraints

Eliot D. Aretskin-Hariton[*], Aaron J. Swank[†], Justin Gray[‡]

NASA Glenn Research Center, Cleveland, OH, USA

Deep-space optical communication will enable increased science return and public engagement for robotic and manned missions. The Integrated Radio and Optical Communication (iROC) project is studying a beaconless optical communication system for Mars data downlink. A star tracker provides the optical communications pointing information in place of an uplink targeting beacon. The configuration presented in this paper includes a star tracker that is aligned co-boresighted with the optical communication axis. This co-boresight configuration was not discussed in prior work, as it was assumed that large Sun-Probe-Earth keep-out angle requirements for operation of the star tracker would cause significant communication outages. In this paper it is shown that the use of an optimal mechanical mounting angle combined with an advanced star tracker has the capability to yield up to 92% communication availability for an example five-year Mars mission.

Nomenclature

Acronyms

FOV	field of view
GMAT	General Mission Analysis Tool
IMU	inertial measurement unit
iROC	Integrated Radio and Optical Communication
LCRD	Laser Communications Relay Demonstration
MPE	Mars-Probe-Earth
SC	spacecraft
SEP	Sun-Earth-Probe
SPE	Sun-Probe-Earth
ST	star tracker
XB	cross boresight

I.   Introduction

OPTICAL communication links are a key element to increasing the volume of data retrieved from missions to nearby planets. Data volume refers to the total data successfully downlinked over the course of a mission. Estimates indicate that data requirements will increase by ten-times each decade through 2040's with the current mission plan.[1] Future robotic missions to Mars will take advantage of the maximum possible communication bandwidth to support science return. Manned missions to Mars have an added requirement of being able to support high-definition video streams to maximize public engagement and ensure constant communication with the astronauts. The Integrated Radio and Optical Communication (iROC) project seeks to support these communication requirements by studying optical communications platforms that can be deployed at Mars distances.[2,3] For this paper, a concept was developed for a five-year long mission of

---

[*]Aerospace Technologist
[†]Research Engineer
[‡]Aerospace Technologist

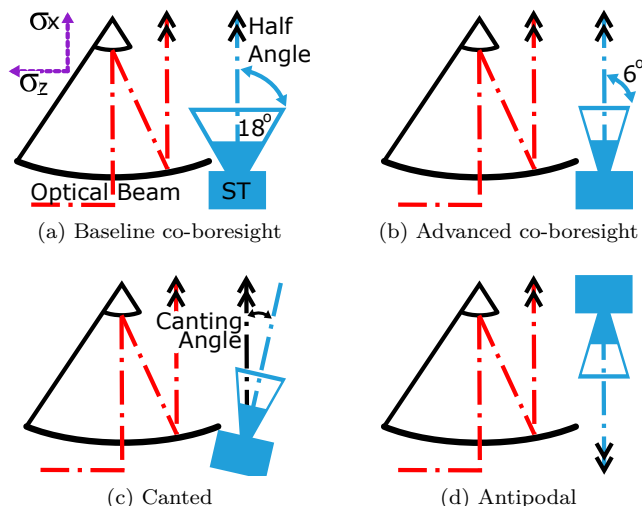American Institute of Aeronautics and Astronautics

Figure 1: Potential iROC configurations showing star tracker and primary and secondary mirrors in a Cassegrain configuration: (a) Baseline iROC co-boresight system with standard star tracker. (b) Co-boresight with advanced star tracker. (c) Advanced star tracker canted away from the optical beam. (d) Antipodal configuration with advanced star tracker facing opposite the optical beam.

an areostationary spacecraft (SC). Such an orbiter would be ideal for a space-based relay for data downlink from Mars to Earth.

Several types of deep-space optical communication configurations have been published in the literature.[2, 4, 5] The configurations in this work are based on the iROC beaconless communications concept,[2] where a star tracker is used to provide the optical communications pointing information instead of an uplink beacon.[6] The iROC concept is distinct from the majority of the other concepts described in the literature, as no uplink tracking beacon is used to provide the necessary pointing information. Instead, this information is provided by the star tracker attitude estimate. The four beaconless configurations discussed in this paper are: the baseline co-boresight system with a standard star tracker (ST); a co-boresight system with an advanced ST; a canted system with an advanced ST; and the antipodal ST configuration. Figure 1 provides a graphical depiction of the beaconless configurations discussed.

Concerns about the co-boresight design stem from the inability to communicate for small Sun-Probe-Earth (SPE) angles.[4] Depending on the ST field of view (FOV) a portion of the contact time may be lost to ST detector saturation when the Sun is within the ST FOV. This research shows that co-boresight and canted configurations are viable. Two methods are used in this approach: i. the use of an advanced star tracker with a $6°$ Sun-Earth-Probe (SEP) half-angle keep-out (Figure 1b), and ii. canting or tilting the advanced star tracker slightly away from the outgoing communication beam axis (Figure 1c). Both of these methods will allow the ST to operate with smaller SPE angle constraints and increase the volume of data returned. Yet, canting the star tracker away from the communication beam axis typically decreases the accuracy of the attitude solution along that direction.

This paper will investigate the trade-off between increasing contact time and decreasing the attitude solution accuracy to ensure that overall, an improvement in data volume is achieved. Sec II covers the methods used to evaluate canting the ST. Sec III covers creation of the simulation which models the communication availability, including the use of General Mission Analysis Tool (GMAT)[7] to determine limitations on availability. Sec IV discusses the formulation of the throughput ratio and how small changes in ST pointing angle can lead to small decreases in accuracy but large increases in availability, leading to an overall increase in data volume. Sec V contains a discussion, and error analysis. Conclusions are presented in Sec VI.

II.   Pointing Accuracy Analysis

Canting or tilting the star tracker away from the communication axis is one of the key tools used in this analysis to increase communications availability. An analysis of the accuracy change in terms of cant

angle will be constructed in order to determine the effects of accuracy and availability on data volume. An example based on an assumed set of iROC system parameters will be used in the analysis.

The beam direction estimate produced by the SC is constructed using inputs from the attitude estimation system and elements of the optical system. The estimate is typically described as a combination of jitter errors and bias errors. The iROC system includes, for example, a navigation grade inertial measurement unit (IMU) and advanced ST,[3] as well as optical components such as a hollow retro-reflector.[8] The final error covariance matrix Σ is typically equal about the two cross boresight (XB) axes, and the largest error is about the roll axis of the ST. The error covariance matrix[a] can be described as:

$$\Sigma = \begin{bmatrix} \sigma_x\sigma_x & 0 & 0 \\ 0 & \sigma_y\sigma_y & 0 \\ 0 & 0 & \sigma_z\sigma_z \end{bmatrix} \tag{1}$$

where the x-axis points down the boresight of the star tracker, and the y and z-axes are the XB components of the error. The coordinate system is shown in Figure 1a with σ_y going into the page, completing the right-handed coordinate frame. The attitude solution variance about the roll axis is $\sigma_x\sigma_x$, and the variance about the XB axes are $\sigma_y\sigma_y$ and $\sigma_z\sigma_z$. To simulate the effects of canting, the covariance matrix is rotated about the y axis. The corresponding rotation matrix T for a rotation about the y axis is given by:

$$T = \begin{bmatrix} cos(\alpha) & 0 & -sin(\alpha) \\ 0 & 1 & 0 \\ sin(\alpha) & 0 & cos(\alpha) \end{bmatrix} \tag{2}$$

where α is the angle by which the ST is canted. Applying the linear transformation, Equation 2, to the error covariance matrix, Equation 1, one obtains an expression for the covariance matrix rotated by angle α about the y axis:

$$\Sigma_{rot} = T\Sigma T^T \tag{3}$$

When the cant angle is zero, σ_y and σ_z will be nearly identical. As the cant angle is increased, there will be a small difference between the two axes as the distribution becomes more elliptical.

Given the covariance matrix, the probability that the communications beam will successfully hit a target can be described by the bivariate distribution.[9] The radius of the bivariate normal distribution indicates how far the beam is off the target. A circularization method can be applied to the bivariate normal distribution to allow for the comparison of the two XB error terms and return the effective error radius.[10] The method works well when the errors are of similar order of magnitude, as the elliptical distribution is approximated with the geometric mean of the standard deviations:

$$\overline{\sigma} = \sqrt{\sigma_y\sigma_z} \tag{4}$$

Where $\overline{\sigma}$ is the standard deviation of the attitude error and σ_y and σ_z are the standard deviations of the XB error.

A. Results

As an example, assume that the iROC system has 1σ standard deviations of $\sigma_x = 5.2\,\mu\mathrm{rad}$, $\sigma_y = \sigma_z = 1.3\,\mu\mathrm{rad}$. The corresponding error covariance is:

$$\Sigma = \begin{bmatrix} 27.1 & 0 & 0 \\ 0 & 1.6 & 0 \\ 0 & 0 & 1.6 \end{bmatrix} \mu\mathbf{rad}^2$$

Using Equation 3 and 4, the cumulative error in the XB as a result of the circularization approximation is shown in Table 1 for various cant angles. From Table 1, it is seen that the attitude estimation error increases only slightly for small cant angles.

---

[a]For simplicity, the variance/covariance matrix is referred to as simply the 'covariance matrix'.

American Institute of Aeronautics and Astronautics

Table 1: Communication beam attitude error estimated via circularization method and shown as a percent increase from zero cant angle.

Attitude Error	Cant Angle (deg)						
	0	1	2	3	4	5	6
1σ Error (μrad)	1.279	1.281	1.285	1.293	1.303	1.316	1.331
Percent Increase (%)	0	0.1185	0.4712	1.051	1.844	2.837	4.009

III. Communication Availability Analysis

Availability of a communication system is the time during which the system is capable of transmitting data. In order to analyze the communications availability, a notional optical communication system is assumed and a SC orbit is simulated using the GMAT. Simulation parameters are presented in Table 2. The orbit is propagated for five years starting on the 1st of January, 2030. The orbit is areostationary, designed to provide continuous orbital coverage for a manned Mars mission.

GMAT is used to calculate the time history of SPE, SEP, and Mars-Probe-Earth (MPE) angles every 10 minutes for the entire five-year interval. These angles are illustrated in Figure 2. Values for the ST FOV, the ground station FOV, and apparent Mars angle while in areostationary orbit are used in post-processing to determine availability of the optical link. The assumption is made that as long as the optical beam can reach Earth, there will always be an available ground station. Currently the required infrastructure to ensure continuous ground station availability does not exist. It is assumed that a manned Mars mission would precipitate its construction.

Table 2: Simulation Parameters

Parameter	Value
Date Format	TAIModJulian
Epoch	32503
Coordinate System	MarsBodyInertial
SMA (a)	20427.6 (km)
ECC (e)	0
INC (i)	0
RAAN (Ω)	0
TA (ν)	82.0°
Propagation duration	5 (years)
Step size	10 (min)
Ground Station field of view	5°(half angle)
Apparent Mars Angle in areostationary Orbit	9.42°(half angle)
Star Tracker field of view	18°or 6°(half angle)

There are several geometric configurations of the Earth, Sun, SC, and Mars that limit the ST's ability to see stars and determine the attitude of the SC in the inertial frame. GMAT assists in calculating these angles which include SEP, SPE, and MPE. When the SPE angle is small, the Sun is within the exclusion angle of the ST. The photons from the Sun then saturate the detector, preventing the ST from observing the faint stars necessary for an attitude solution. A second type of limitation happens when Mars is within the FOV of the ST, creating a Mars eclipse. Photons from the surface of Mars shine into the ST, preventing it from achieving an attitude solution. This typically happens when MPE is small but with the antipodal star tracker (Figure 1d) this occurs when MPE is large. Additionally, with the antipodal star tracker configuration, it is possible for Mars to obstruct the optical beam between the SC and Earth even when the ST has an attitude solution. Finally, if SEP angle is less than 5 °, it is assumed that Earth-based detectors will be unable to pick out the laser signal a midst the background noise of the Sun. This assumption is consistent with the Optical Ground Station-1 keep-out angle.[5]
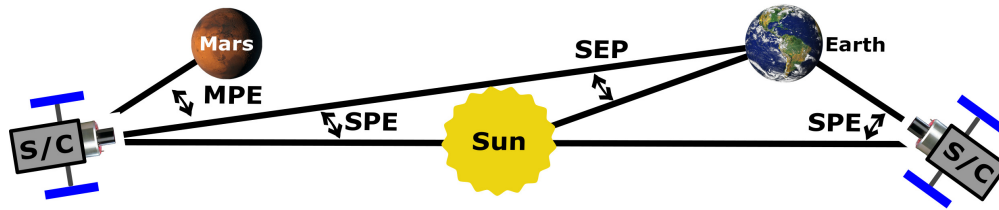
Figure 2: Illustration of angles resulting in limited communication availability as modeled in GMAT: Sun in ST FOV (SPE), Sun in Ground Station FOV (SEP), Mars in ST FOV or Mars in the communication beam line of sight (MPE).

A.   Results

Data was produced for the four configurations described in Section I. The results of availability vs. canting angle as produced by GMAT are shown in Table 3. The canted system was rotated from zero to $6°$ and is shown in the the advanced ST row. It should be noted that the results are strongly dependent on the input parameters. For example, the ST FOV half angle of $6°$ will prevent canting further than this angle. Additionally, stars on the edge of the ST are often not used, due to optical distortions. Therefore, it is assumed that canting should be restricted to at least one degree less than the maximum ST FOV half angle. So while there is an improvement shown by the entries in Table 3, the physical limit of the $6°$ FOV system is at $5°$.

Table 3: SC Communication availability % depending on ST and cant angle.

Configuration	FOV	Cant Angle (deg)						
		0	1	2	3	4	5	6
Baseline ST	$18°$	55.9	-	-	-	-	-	-
Advanced ST	$6°$	85.5	87.5	89.5	91.3	91.4	91.6	91.7
Antipodal ST	$6°$	90.6	-	-	-	-	-	-

The availability results for the baseline star tracker with an $18°$ half angle baffle mounted co-boresight is shown in Figure 3a. The three most important metrics for measuring availability (MPE, SPE, and SEP) are shown individually. SEP angle causes a communication outage from approximately day 30 to day 250. During this time, the Sun is between Earth and Mars which prevents the ST from acquiring an attitude solution. SEP angle causes a communication outage from approximately day 460 to day 510. During this time, the Earth is between Mars and the Sun so the ST looks towards Earth and is therefore blinded by the Sun. MPE angle causes intermittent communication outages every day for the whole mission. This occurs when Mars slips in and out of the ST FOV, blocking an attitude solution. The effects of reducing the star tracker FOV, as shown in Figure 3, will directly affect how often the Sun is within the ST FOV.
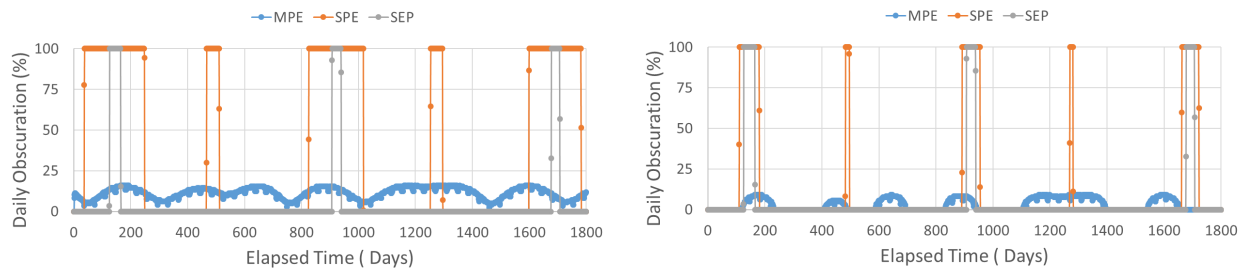
(a) Standard 18° FOV Star Tracker, daily obscuration % during a 5 year mission.

(b) Advanced 6° FOV Star Tracker with no canting, daily obscuration % during a 5 year mission.

Figure 3: GMAT output graphs for a year five long Mars areostationary orbit simulation. Minimizing the area under the curve yields increased contact time and increased data volume.

American Institute of Aeronautics and Astronautics

IV. Data Volume Calculations

In the previous two sections, models were given for the pointing accuracy of an optical communication system and the overall availability of the system. Both models were presented as a function of how far the ST is canted from the communications beam boresight direction. To understand the optimal canting angle, it is necessary to calculate data volume as a function of cant angle. Additionally, the optimal canting angle will be applied to an example problem to demonstrate the application of this concept.

A. Calculations

Given a nominal data volume T_o of the communication system at zero cant angle, the data volume T_α at a selected cant angle α can be calculated as:

$$\frac{T_\alpha}{T_o} = \frac{w_\alpha}{w_o} \tag{5}$$

where w_o is a reference scale factor at zero cant angle, and w_α is the scale factor at the selected cant angle α. The scale factors w_o and w_α are constructed using the knowledge that data volume is directly correlated with availability (the more time available to transmit leads to more data being sent to Earth). In addition, data volume is inversely proportional to pointing accuracy (poor pointing accuracy leads to missing the target ground station). Therefore, w_o and w_α are constructed as follows:

$$w_o = \frac{Av_o}{Ac_o}, \; w_\alpha = \frac{Av_\alpha}{Ac_\alpha} \tag{6}$$

where Av_o is the availability (%) at zero cant angle, and Ac_o is the pointing accuracy (μrad) at zero cant angle. These fractions can be calculated and then combined to create the throughput ratio R_α:

$$R_\alpha = \frac{w_\alpha}{w_o} = \frac{Av_\alpha}{Ac_\alpha} \times \frac{Ac_o}{Av_0} \tag{7}$$

Finally, an expression for the data volume in terms of cant angle is created by combining Equation 5 and Equation 7:

$$T_\alpha = T_o \times R_\alpha \tag{8}$$

where T_o is the nominal data volume of the system at zero cant angle and R_α is the throughput ratio given by Table 4.

Table 4 shows the throughput ratio, Equation 7, as a function of the pointing accuracy and communication availability using information from Table 1 and 3. It can be seen that the pointing accuracy (Ac_α), which is given as a standard deviation, increases as ST cant angle increases. This means that the circle bounding the optical system pointing direction is getting larger as cant angle increases and corresponds with a decrease in the probability that a photon will land on the ground detector. However, there is a significant increase in availability as cant angle increases. If the increase in availability outweighs the accuracy degradation, an overall increase in data volume will result in a throughput ratio (R_α) larger than 1. Values below 1 indicate that data volume has decreased. The change in data volume as a function of cant angle is also plotted in Figure 4.

B. Example

The effect of the throughput ratio (R_α) on a SC configuration can be seen in the following example. Consider a co-boresight beaconless optical system (Figure 1b). This system is designed to send 100 Tbits of information (data volume) from Mars to Earth over a five year mission. To determine the resulting data volume that could be downlinked if the ST was canted at $3\,^\circ$ (Figure 1c), select the corresponding R_α from Table 4 and apply that value to Equation 8 as follows:

$$T_\alpha = T_o \times R_\alpha = 100 \times 1.057$$

The final result is that the data volume would increase to 105.7 Tbits over the five year mission when the system is canted at $3\,^\circ$. This indicates that all other things being equal, the canted system performs better than the co-boresight system.

American Institute of Aeronautics and Astronautics

Table 4: Throughput ratio (R_α) for SC optical communication system with advanced ST (6° FOV). Corresponding availability (Av) and accuracy (Ac) values also included.

Parameter	Cant Angle (deg)						
	0	1	2	3	4	5	6
Av_α (%)	85.5	87.5	89.5	91.3	91.4	91.6	91.7
Ac_α ($\mu rad, 1\sigma$)	1.279	1.281	1.285	1.293	1.303	1.316	1.331
R_α (ratio)	1.0	1.022	1.042	1.057	1.050	1.041	1.031

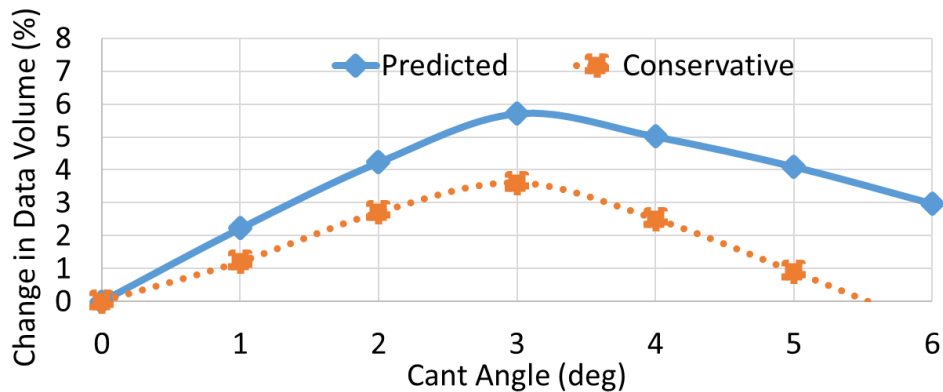
Figure 4: Change in data volume ($1 - R_\alpha$) shown as a function of cant angle for SC optical communication system with advanced ST (6° FOV). Conservative estimate is discussed in Section V.B.

V. Discussion

A. Configuration Estimated Performance

The evaluation of the primary system configuration options and relevant constraints will be discussed. Those considered are the limitations imposed on the ST FOV, the orientation of the ST on the spacecraft relative to the outgoing communications laser beam direction, and finally a brief discussion on the comparison of a beaconless to a beacon-aided configuration in terms of overall communications availability.

1. Dependence on ST FOV

The communication availability results for a beaconless optical communication system using the co-boresight configuration and a standard STs with a large 18° FOV were shown in Table 3. The availability for this configuration is very low (56%), which is consistent with expectations from previous research.[4] The amount of lost contact time due to limitations in SPE, SEP, and MPE angles is shown in Figure 3a. As indicated by Figure 3a, the majority of the lost contact time is due to the SPE angle limitation. Thus, by reducing the overall FOV for the ST, the amount of contact time lost due to SPE angle limitations would be reduced. As an example, consider the advanced ST with a small 6° FOV in the same co-boresight configuration. The communication availability values shown in Table 3, indicate much improved results with availability increasing to almost 86% for the 6° FOV configuration. This also corresponds to Figure 3b where now the total amount of lost contact time attributed to SPE angle and SEP angle limitations are much closer matched. It is noticeable that the SPE angle limitation is still the largest contributor to the overall loss in communication availability, but now the contribution due to the SEP limitation is now comparable in magnitude. The results are also in agreement with the Optical Link Study Group (OLSG)[6] report which indicates that for SPE angles of 6°, the matching SEP angle is 8.6°. Since the SEP angle used for the simulations in this work is 5°, the FOV of the ST could be decreased slightly before the limiting factor in overall communications availability becomes the ground station.

2. *Dependence on ST Cant Angle*

The results from canting the advanced ST FOV configuration away from the laser communications beam boresight direction can also be seen in the third line of Table 3. It is noticeable that the availability increases for a cant angle range from $0°$ to $3°$ and then decreases slightly thereafter. The observed decrease in the communications availability corresponds with the dominant factor switching from the limitation in SPE angle to the SEP angle. Because canting the star tracker increases the accuracy error and therefore degrades the performance of the overall pointing system, a throughput ratio for the canted system (as described in Section IV) was used to estimate the change in total availability over the five-year mission as compared to the non-canted reference case. This throughput ratio (R_α) is shown in the last row of Table 4. The system experiences a change in the throughput ratio by up to 5.7% from the baseline before decreasing slightly to 3.1%. The observed trend corresponds with an increase in availability from a cant angle of $0°$ to $3°$. After a $3°$ cant angle, availability increase is minimal but accuracy error continues to increase, outweighing the benefits from marginal availability increases. Therefore, a cant angle does exist which can optimally increase data volume.

3. *Antipodal Aligned ST Versus Co-boresight Aligned*

The antipodal configuration with the advanced ST (Figure 1d) is listed in the fourth line of Table 3 and shows good availability results. However, 90.6% availability is less than the capabilities of the advanced ST when it is canted at $3°$. The active constraint in the system is the earth ground station as seen in Figure 3b. Thus, while the antipodal configuration may provide additional capability to transmit without being blinded by the Sun, the ground station does not have the capability to receive that signal. Based on OLSG report,[6] the Antipodal case would only provide more availability once ground stations could handle SEP angles of less than $2.8°$.

4. *Comparison to Beacon-Aided Laser Communication*

Constraints on beacon-aided systems differ greatly from those of beaconless systems.[3] It is estimated that a beacon-aided system for Earth to Mars distances would require the use of a $5\,\mathrm{kW}$ ground-based laser beacon.[6] A powerful uplink beacon could interfere with aircraft overflight, creating large no-fly zones around each ground terminal. The laser beacon may also interfere with ground-based science observation campaigns.[6] Thus while beacon-aided Mars downlink systems with similar capability to the Laser Communications Relay Demonstration (LCRD) flight payload have an estimated availability of 93%, the actual availability for a long-duration mission is expected to be lower. Beaconless systems do not suffer from the aforementioned constraints. Yet, the presented configuration employing a canted ST does impose constraints on SC concept of operations. When SPE angles become small, the optical platform or the SC must rotate $180°$ around the Sun-Probe axis to maximize the availability, which is listed in Table 4. This geometric configuration occurs approximately once per year and is therefore likely a minor inconvenience to the overall concept of operations.

B. Model Simplifications and Uncertainties

Model simplifications and uncertainties for the study may be placed into three categories: model simplifications that are accounted for in the simulation, uncertainties that are deemed negligible, and finally those uncertainties which were not examined in detail for this work.

1. *Simplifications Included*

The attitude error values shown in Table 1 were approximated using a circularization technique. The technique estimates an elliptical distribution with a circular distribution and therefore creates small errors. For standard deviation ratios of $0.8 \leq \sigma_y/\sigma_z \leq 1.2$ it can be shown that these errors are less than 0.5%. During the analysis presented in this paper, the ratio stayed between 1 and 0.96. The conservative estimate shown in Figure 4, includes an estimation for this simplification.

The availability calculations for canting the spacecraft presented in Table 3 were simplified to only affect SPE angles, whereas in a real system canting would also affect MPE angles. The simplification assumed that canting away from the Sun would not cause the ST to cant into Mars. By making this simplification the analysis focused on the overall geometric constraints rather than a detailed controls analysis. The resulting

error from the simplification can be bounded by enlarging the ST FOV by the cant angle when performing MPE angle checks only. The resulting effect is a scenario whereby one assumes that the ST is always canted in a direction closer towards Mars. The conservative estimate shown in Figure 4, includes an estimation for this simplification.

2. Negligible Uncertainties

Relativistic effects of light travel time are neglected in this analysis. While GMAT does provide the ability to place ground stations and to check contact times with relativistic compensation, additional post processing would have been required outside of GMAT. Previous studies suggest that these effects may require pointing ahead by up to $400\,\mu$rad.[6] This is considered too small to effect the overall availability, which is only significantly affected by changes on the order of degrees.

Line of sight irruptions from Mercury, Venus, or moons including Luna, Phobos, and Deimos, are not considered in this analysis. It is expected that these effects would have only very small effects on availability and would not effect the rational for canting.

Cyclical variation in SEP and SPE angles independently cause communication outages. A change of mission duration or mission start date may cause more or fewer outages during the mission. During the five-year mission there are five outages caused by these effects. If the mission had started 200 days later a 95 day outage near the start of the mission would have been skipped. Over the mission length of 1824 days, avoiding this outage would have resulted in an increase of availability for all scenarios in Table 3 of approximately 5%. Yet, the relative change between the baseline co-boresight case and canted cases is expected to be small.

The calculations for MPE angle assume that when the edge of Mars is within the half-angle of the star tracker, the attitude solution is immediately lost. This may be an overly conservative approach. While Mars shine may be an issue, it is conceivable that stars would still be visible in the ST FOV even if Mars was partially obscuring that FOV. Additionally, the IMU would still propagate the attitude information, which could preserve the pointing solution for a time. These effects could increase availability slightly in all examined cases.

The calculation of SEP, SPE, and MPE angles were performed at ten minute intervals. This could lead to an error in availability based on the number of transitions between available and unavailable. Since on average only two transitions happen per day, the availability could be off by as much as $\pm1.4\%$ for a single day. However the average error is very close to zero for a 1,000+ day mission, and therefore does not significantly effect our results in Table 3.

3. Unquantified Uncertainties

Data rates achievable by the system are subject to variations in SEP angle.[11] When the angle is small, the ground station is operating close to the sun which causes the background sky to be brighter. This will make it harder to detect incoming light from the SC. A weighting factor was not included for this effect, making this a relevant area for future work.

VI. Conclusion

A beaconless laser based optical communication system for Mars to Earth high volume data downlink was described. Four system configurations were analyzed, including: standard star tracker (ST) mounted co-boresight to the communication beam, an advanced ST mounted co-boresight, a canted advanced ST, and an antipodal advanced ST. Communications availability of each system for a nominal five-year Mars mission was conducted. The accuracy of the attitude solution was also evaluated as a function of cant angle. An assessment of data volume successfully downlinked to Earth was created as a function availability and accuracy. The optimal configuration was found by canting the advanced ST 3° off-boresight. This increased the availability to 91.3% at the expense of decreasing accuracy by 1.1%. The resulting data volume demonstrated a 5.7% increase compared to the co-boresight advanced ST. A once-per-year concept of operations penalty is incurred as a result of selecting the canted system. It is estimated that a beaconless optical communication platform with an advanced ST canted at 3° can perform on the order of current beacon-aided systems which are estimated to have availability in the range of 92.6%.

Acknowledgements

References

[1] Deutsch, L., "Meeting the Communications Challenges of NASA's Future Deep Space Missions," *Proceedings of the 22nd Annual KA and Broadband Communications Conference*, Jet Proplulsion Lab, Pasadena, CA, October 2016.

[2] Raible, D., Romanofsky, R., Budinger, J., Nappier, J., Hylton, A., Swank, A. J., and Nerone, A. L., "On the Physical Realizability of Hybrid RF and Optical Communications Platforms for Deep Space Applications," *32nd Inernational Communications Satellite Systems Conference*, AIAA, San Diego, CA, 2014.

[3] Swank, A. J., Aretskin-Hariton, E., Le, D. K., Sands, O., and Wroblewski, A., "Beaconless Pointing for Deep-Space Optical Communication," *34th AIAA International Communications Satellite Systems Conference*, 2016.

[4] Ortiz, G. G. and Lee, S., "Star Tracker Based ATP System Conceptual Design and Pointing Accuracy Estimation," February 2006.

[5] Edwards, B. L., Israel, D., Wilson, K., Moores, J., and Fletcher, A., "Overview of the Laser Communications Relay Demonstration Project," 2012.

[6] Interagency Operations Advisory Group, Optical Link Study Group, "Optical Link Study Group Final Report," IOAG.T.OLSG.2012.V1, June 2012.

[7] The GMAT Development Team, "GMAT User Guide R2017a," National Aeronautics and Space Administration, 2017.

[8] Swank, A. J. and Aretskin-Hariton, E., "The influence of dihedral angle error stability on beam deviation for hollow retro-reflectors," *TM-2018-219946*, 2018.

[9] Bertsekas, D. P. and Tsitsiklis, J. N., *Introduction to Probability, 1st Edition*, Athena Scientific, Belmont, MA, 2002.

[10] Lanzi, J., "Notes on Mathematics of Impact Dispersion and Normal Bivariate Distributions," *personal correspondents*, 2017.

[11] Boroson, D. M., "On Achieving High Performance Optical Communications from Very Deep Space," *SPIE*, Vol. 10524, No. 105240B-1, 2018.